Available online at www.sciencedirect.com

ScienceDirect

Biochimie Open 1 (2015) 61–69

www.elsevier.com/locate/biopen

Research paper

Identification of a nicotinamide/nicotinate mononucleotide adenylyltransferase in *Giardia lamblia* (GlNMNAT)

Nicolás Forero-Baena, Diana Sánchez-Lancheros, July Constanza Buitrago, Victor Bustos, María Helena Ramírez-Hernández*

Department of Chemistry, Universidad Nacional de Colombia, Bogotá Cundinamarca, Colombia

Received 9 April 2015; received in revised form 18 October 2015;Available online 18 November 2015

Abstract

Giardia lamblia is an intestinal protozoan parasite that causes giardiasis, a disease of high prevalence in Latin America, Asia and Africa. Giardiasis leads to poor absorption of nutrients, severe electrolyte loss and growth retardation. In addition to its clinical importance, this parasite is of special biological interest due to its basal evolutionary position and simplified metabolism, which has not been studied thoroughly. One of the most important and conserved metabolic pathways is the biosynthesis of nicotinamide adenine dinucleotide (NAD). This molecule is widely known as a coenzyme in multiple redox reactions and as a substrate in cellular processes such as synthesis of Ca^{2+} mobilizing agents, DNA repair and gene expression regulation. There are two pathways for NAD biosynthesis, which converge at the step catalyzed by nicotinamide/nicotinate mononucleotide adenylyltransferase (NMNAT, EC 2.7.7.1/18). Using bioinformatics tools, we found two NMNAT sequences in *Giardia lamblia* (*glnmnat-a* and *glnmnat-b*). We first verified the identity of the sequences *in silico*. Subsequently, *glnmnat-a* was cloned into an expression vector. The recombinant protein (His-GlNMNAT) was purified by nickel-affinity binding and was used in direct *in vitro* enzyme assays assessed by C18-HPLC, verifying adenylyltransferase activity with both nicotinamide (NMN) and nicotinic acid (NAMN) mononucleotides. Optimal reaction pH and temperature were 7.3 and 26 °C. Michaelis–Menten kinetics were observed for NMN and ATP, but saturation was not accomplished with NAMN, implying low affinity yet detectable activity with this substrate. Double-reciprocal plots showed no cooperativity for this enzyme. This represents an advance in the study of NAD metabolism in *Giardia* spp.

Keywords: *Giardia lamblia*; NMNAT; NAD metabolism; Enzyme activity.

1. Introduction

Nicotinamide adenine dinucleotide (NAD) is a key molecule in cellular metabolism [1]. Its central role as a coenzyme in REDOX reactions has been known since its function as an acceptor and donor of hydride ions was established [2], which is an essential characteristic for the maintenance of cellular REDOX balance and energy production. In addition, NAD is used as substrate in non-REDOX reactions, e.g., deacetylation by sirtuins [3], mono and poly-ADP-ribosylation [4,5] and the synthesis of key second messengers in Ca^{2+} mobilization such as nicotinic acid-adenine dinucleotide phosphate (NAADP), cyclic ADP-ribose (cADP), ADP-ribose (ADPR) [6] and O-acetyl-ADP-ribose (OAADPR) [7]. These non-REDOX reactions are part of fundamental cellular processes, e.g., gene expression regulation, DNA repair, chromatin stability, calcium mobilization, circadian rhythm control and cell death [2,8]. When used as a coenzyme in oxidation–reduction reactions, NAD exists in its oxidized form NAD^+ and in its reduced form NADH, maintaining a constant concentration. However, in non-REDOX reactions

Abbreviations: QAPRT, quinolinic acid phosphoribosyltransferase; NAPRT, nicotinic acid phosphoribosyltransferase; NAMPRT, nicotinamide phosphoribosyltransferase; NRK, nicotinamide riboside kinase; NMNAT, nicotinamide/nicotinic acid mononucleotide adenylyltransferase; NAD synthetase, EC. 6.3.5.1; QA, quinolinic acid; NA, nicotinic acid; NAM, nicotinamide; NR, nicotinamide riboside; NAMN, nicotinic acid mononucleotide; NMN, nicotinamide mononucleotide; NAAD, nicotinic acid adenine dinucleotide; NAD, nicotinamide adenine dinucleotide.

* Corresponding author.
E-mail address: mhramirezh@unal.edu.co (M.H. Ramírez-Hernández).

http://dx.doi.org/10.1016/j.biopen.2015.11.001

in which NAD undergoes chemical breakdown, it is consumed, reducing its concentration.

Given this scenario, the cell must have NAD biosynthetic pathways to maintain a constant source of this molecule. There are two main NAD biosynthetic pathways (Fig. 1): one *de novo* pathway from quinolinic acid (QA) and a salvage pathway from nicotinamide (NAM), nicotinic acid (NA) and nicotinamide riboside (NR). Both the *de novo* pathway and the salvage pathway converge in NMNAT catalytic activity, which involves the Mg^{2+}-dependent reversible condensation [9,10] of ATP with NMN (nicotinamide mononucleotide) or NAMN (nicotinate mononucleotide), producing NAD (nicotinamide adenine dinucleotide) or NAAD (nicotinate adenine dinucleotide), respectively [11]. Ubiquitous in nature, this enzyme has been found in all organisms from all three kingdoms of life (archaea, eubacteria, eukaryotes) in which it has been sought, justifying the importance of its function in the cell.

The present study aims to examine NAD metabolism in the parasitic protozoan pathogen *Giardia lamblia* (also called *Giardia intestinalis* or *Giardia duodenalis*) through the identification, cloning, expression, purification and enzymatic validation of nicotinamide/nicotinate mononucleotide adenylyltransferase (NMNAT), which was identified using bioinformatics tools.

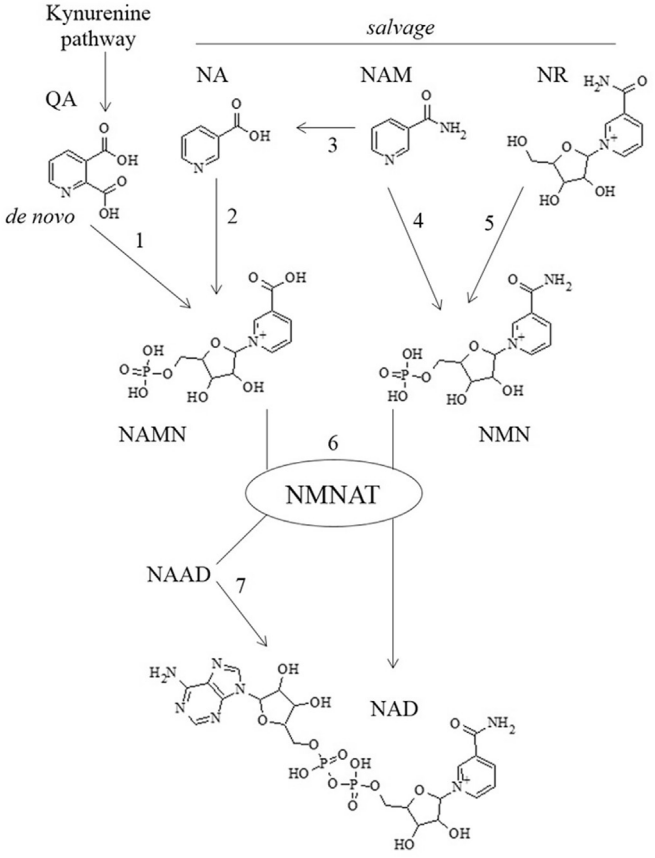

Fig. 1. **Representation of NAD biosynthesis**. Enzymes involved are denoted by numbers: 1. QAPRT (quinolinic acid phosphoribosyltransferase, EC. 2.4.2.19). 2. NAPRT (nicotinic acid phosphoribosyltransferase, EC. 2.4.2.11). 3. Nicotinamidase (EC. 3.5.1.19). 4. NAMPRT (nicotinamide phosphoribosyltransferase, EC. 2.4.2.12). 5. NRK (nicotinamide riboside kinase, EC. 2.7.1.22). 6. NMNAT (nicotinamide/nicotinic acid mononucleotide adenylyltransferase, EC. 2.7.7.1/18). 7. NAD synthetase (EC. 6.3.5.1). Images drawn with ChemSketch Freeware (ACD/Labs v14.01).

2. Materials and methods

2.1. Identification and bioinformatic validation of the putative sequence

Multiple sequence alignment of 16 NMNAT sequences reported in the UniProtKB database (http://www.uniprot.org/) was performed using the MUSCLE [12,13] algorithm in the CLC Sequence Viewer v6.9 (Additional Alignments plugin v.1.4.5) program. The resulting consensus sequence of 244 aa was used to search the GiardiaDB [14] (http://giardiadb.org/giardiadb/) using the BLAST algorithm. The sequences with the highest score and lowest E-value were subsequently validated by finding conserved domains and their putative function. Additionally, a 3-dimensional model of the putative protein was obtained (I-TASSER server [15,16]) to compare it with the structure of crystallized and reported NMNATs.

2.2. Culture of Giardia lamblia

Parasites (WB clone C6) were cultured in borosilicate tubes at 37 °C in TYI-S-33 medium (Diamond, 1978). Subsequently, the parasites were separated from the medium by centrifugation (1500 rpm, 10 min) and washed three times with cold sterile PBS. The washed parasites were resuspended in 6 mL of sterile PBS and counted in a Neubauer chamber. The parasites were centrifuged again, and the resultant pellet was stored at −20 °C to subsequently extract genomic DNA [17].

2.3. Genomic DNA extraction

Cells (7.5×10^7) were resuspended in 200 μL of sterile PBS. From these cells, genomic DNA was extracted using an Easy-DNA™ kit (Invitrogen). The extracted DNA was resuspended in 100 μL of TE buffer and stored at 4 °C. Purity and concentration were evaluated by a UV–Vis spectrophotometer (Spectronic Genesys 5) at 260 and 280 nm.

2.4. PCR amplification of the coding region

The NMNAT coding region of *Giardia lamblia* was amplified from genomic DNA using the following primers: 5'-caccATGCCCTGTCCGCCGGT-3′(forward) and 5′-TTATTGGAAACTAGGGGGTG-3 (reverse). The amplification conditions were as follows: 3 mM $MgCl_2$, 0.5 μM primers, 0.2 mM dNTPs, 2.5 U of Taq polymerase (Amplitaq) and 100 ng of gDNA template. PCR was performed in a final volume of 25 μL in a GeneAmp® PCR system 2400 Perkin Elmer™ thermal cycler. The optimal thermal cycle used was

Table 1
Reaction mixture for enzyme assays.

Reagent	Volume (μL)	Final concentration
HEPES-KOH pH 7.5 (100 mM)/ $MgCl_2$ (40 mM)	25.0	25 mM/10 mM
ATP (12.5 mM)	10.5	1.31 mM
NMN/NAMN (50 mM)	2.5	1.25 mM
His-GlNMNAT[a]	62.0	60 ng/μL

[a] For the positive control, His-HsNMNAT-3 was used (final concentration in reaction mix: 25 ng/uL). For the negative control, soluble fraction of non-transformed *E. coli* B21 (DE3) cells was used.

as follows: initial denaturation (94 °C, 5 min) followed by 30 denaturation cycles (94 °C, 45 s), annealing (55 °C, 45 s), and extension (72 °C, 1 min) and a final extension at 72 °C for 7 min. The PCR product was evaluated by horizontal electrophoresis in a 1.5% agarose gel in 0.5X TBE buffer. Staining was performed with 0.05% ethidium bromide for 20 min [18]. The gel was visualized on a Molecular Imager® Gel Doc™ XR image analyzer including Quantity One Basic 4.6.3 software from BIO-RAD™.

2.5. Cloning of the amplified coding region into an expression vector

The PCR product (*glnmnat*) was ligated into a pET100/D-TOPO® vector (Champion™ pET Directional TOPO® Expression Kits from Invitrogen™). The resulting recombinant plasmid (pET100/D-TOPO-*glnmnat*) was transformed by heat shock at 42 °C into competent *E. coli* cells (OneShot® TOP10 Competent Cells) [18]. The transformation was confirmed by colony PCR using the primers and thermal program previously indicated.

2.6. Expression vector purification

The pET100/D-TOPO-*glnmnat* expression vector was purified from a 5-mL culture (LB medium + ampicillin) of *E. coli* TOP10 cells previously transformed by the alkaline lysis procedure [18]. Purity and concentration were evaluated using a UV–Vis spectrophotometer (Spectronic Genesys 5) at 260 and 280 nm.

2.7. Transformation into expression strains

The previously extracted recombinant plasmid pET100/D-TOPO-*glnmnat* was transformed into chemically competent *E. coli* BL21 cells (Invitrogen) by heat shock at 42 °C [18].

2.8. Expression of the recombinant protein His-GlNMNAT

Isopropyl-β-D-1-thiogalactopyranoside (IPTG) was added to a 250-mL culture of *E. coli* BL21 ($OD_{600nm} = 0.550$) for a final concentration of 1 mM. Induction was performed at 20 °C with constant stirring for 20 h. After the induction, the culture was centrifuged at 6000 rpm for 10 min at 4 °C, obtaining a bacterial pellet with a wet weight of 1.96 g. The bacterial pellet was resuspended in lysis buffer (50 mM NaH_2PO_4, 300 mM NaCl, 10 mM imidazole, pH 8.0) with 5 mL of buffer per gram of wet solid. Lysozyme was added to a final concentration of 1 mg/mL, as well as ribonuclease (Promega) and protease inhibitor cocktail (Sigma, P8340) at a dilution of 1:400. The mixture was homogenized by vortex stirring and incubated at 4 °C for 2 h. Subsequently, 6 ultrasonic pulses were applied for 15 s followed by a rest of 15 s. The soluble and insoluble fractions were separated by centrifugation at 12,000 rpm for 20 min at 4 °C [18].

2.9. SDS-PAGE and immunoblotting

The soluble and insoluble cell lysate fractions were evaluated by 12% polyacrylamide gel electrophoresis under denaturing conditions (SDS-PAGE) (Coomassie blue staining) [18]. A replica of the gel was transferred to a nitrocellulose membrane (0.45 μm thick; ThermoScientific) in transfer buffer (25 mM Tris base, 192 mM glycine, and 10% methanol v/v) at 200 mA

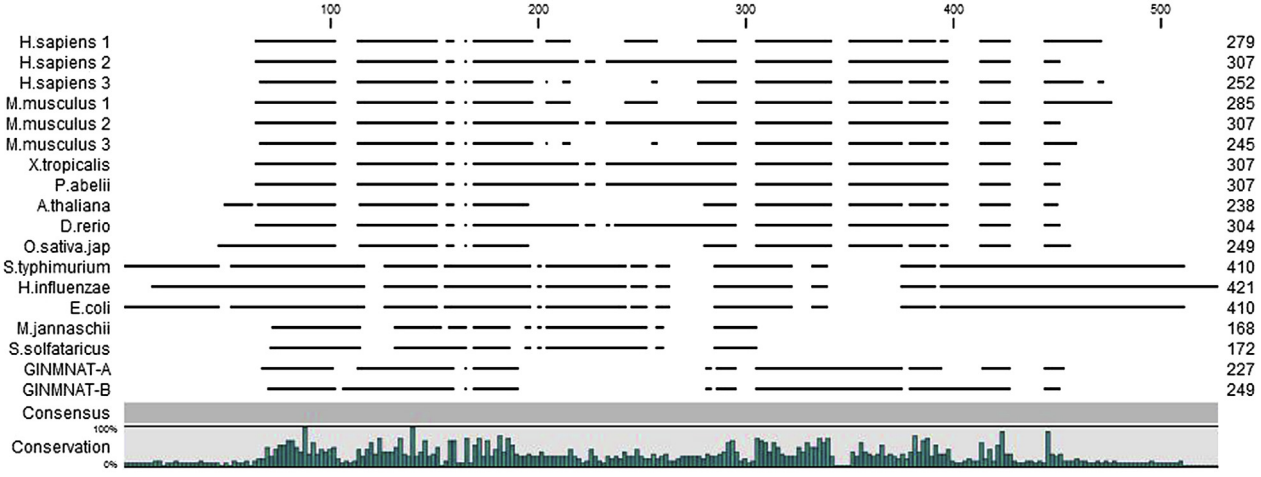

Fig. 2. **Multiple sequence alignment of 16 homologous NMNAT proteins from phylogenetically divergent organisms with GlNMNAT isoenzymes**. The percentage of conservation is displayed throughout the sequence in bars. Alignment was done with the ClustalO algorithm in the CLC Sequence Viewer v7.0.2 program (CLCBio A/S, Additional Alignments plugin v.1.5.1).

for 2 h. The membrane was blocked overnight with a 5% w/v skim milk solution in TBST. Immunodetection of the recombinant protein was performed using a histidine tag with the primary antibody anti-His-mAb (1:3000, Amersham) and secondary antibody anti-mAb-HRP (1:2000); 4-chloro-naphthol (Sigma) and hydrogen peroxide were used as developing agents [19].

2.10. Nickel-affinity purification

Nickel-affinity resin solution (Ni-NTA, Qiagen) was used at 100 μL per milliliter of soluble protein extract. The resin was equilibrated in lysis buffer (50 mM NaH_2PO_4, 300 mM NaCl, 10 mM imidazole, pH 8.0) and incubated with soluble extract

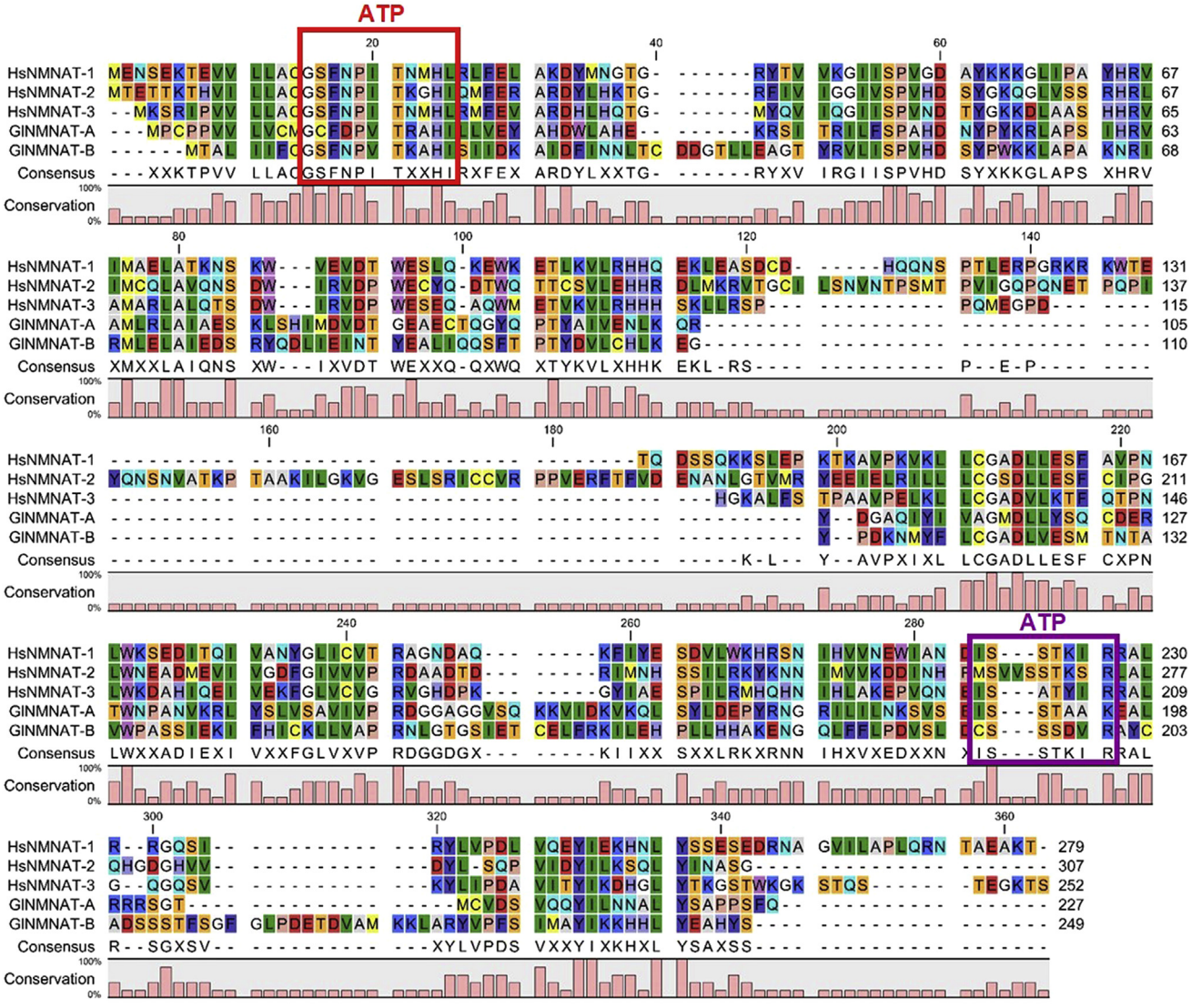

	HsNMNAT-1	HsNMNAT-2	HsNMNAT-3	GlNMNAT-A	GlNMNAT-B
HsNMNAT-1	100	35	51	25	27
HsNMNAT-2	35	100	35	33	33
HsNMNAT-3	51	35	100	25	26
GlNMNAT-A	25	33	25	100	28
GlNMNAT-B	27	33	26	28	100

Fig. 3. **Alignment between the three NMNAT human isoenzymes and the two NMNAT isoenzymes from *Giardia lamblia*.** Conservation percentage per residue position is observed in pink bars. The multiple alignment was done with ClustalO (CLC Sequence Viewer v7.0.2 program, CLCBio A/S, Additional Alignments plugin v.1.5.1). Identity percentages calculated with BLASTP algorithm (NCBI) and shown in the adjacent table. ATP active site motif for recognition and binding in N-terminus and C-terminus regions depicted in red (GxFxPx[H/T]xxH) and violet respectively (ISSTxxR) [10]. (For interpretation of the references to colour in this figure legend, the reader is referred to the web version of this article.)

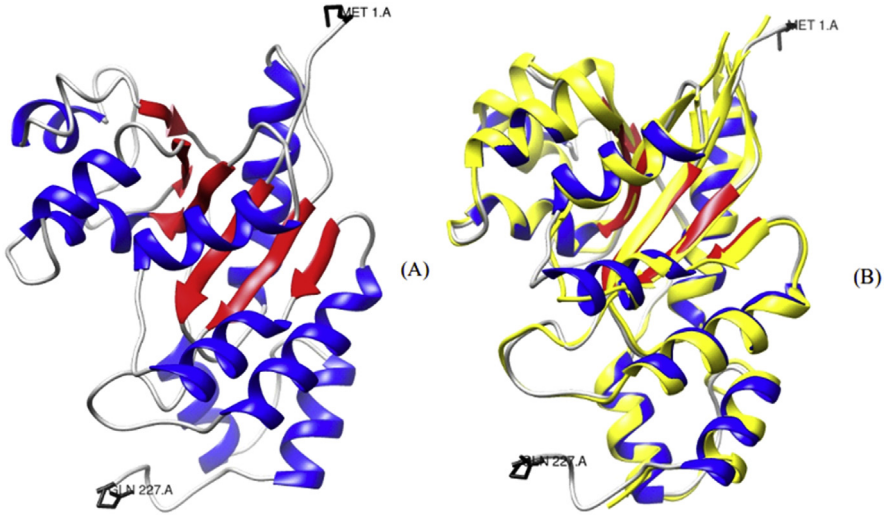

Fig. 4. **GlNMNAT tertiary structure model**. (A) Three-dimensional GlNMNAT model (I-TASSER [15,16]). A Rossmann-type fold, characteristic of nucleotide-binding proteins, is observed. C-score: $-5 < 0.95 < 2$. TM-score: $0.84 \pm 0.08 > 0.5$. RMSD: 3.7 ± 2.5 Å. (B) Overlay of the model with the structure of the HsNMNAT-3 protein (1nuq_A [9], 252 aa, in yellow). Alignment performed with the UCSF Chimera v1.8 program [23]. RMSD between 171 atom pairs: 0.670 Å. Molecular graphics and analyses were performed with the UCSF Chimera package. (For interpretation of the references to colour in this figure legend, the reader is referred to the web version of this article.)

overnight on ice; the supernatant with unbound proteins was collected by centrifugation at 3000 rpm for 3 min. Washes were performed with wash buffer (50 mM NaH_2PO_4, 300 mM NaCl, 20 mM imidazole, pH 8.0) to obtain an absorbance at 280 nm of 0.000 ± 0005. The elution of the recombinant protein was performed with elution buffer (50 mM NaH_2PO_4, 300 mM NaCl, increasing concentrations of imidazole 50 mM/80 mM/250 mM, pH 8.0) on ice overnight. Protein purification was verified by SDS-PAGE and western blotting under previously described conditions [20].

2.11. Evaluation of enzyme activity

An *in vitro* assay was conducted to determine the activity of the purified recombinant protein (Table 1). For the negative control, the elution buffer was used instead of the recombinant protein eluate. For the positive control, an eluate with recombinant *Homo sapiens* NMNAT-3 protein (His-HsNMNAT-3) was used. The mixtures were incubated at 37 °C for 30 min, after which the reaction was stopped with 1.2 M $HClO_4$ at 4 °C. The protein was precipitated by centrifugation at 12,000 rpm for 3 min at 4 °C. The supernatant was neutralized with 1 M K_2CO_3 on ice. A total of 120 μL of supernatant was taken and diluted to 240 μL with MQ H_2O [21].

The resulting product of the *in vitro* reaction was evaluated by reverse phase HPLC. A Phenomenex Luna C18 (250 mm × 4.60 mm, 5 μm) column was used. As mobile phases, 0.12 M potassium phosphate buffer pH 6.0 and methanol were used. The separation was carried out in a gradient (0–8 min 80% buffer 20% water, 8–12 min 0–20% MeOH 80% buffer, 12–14 min 20% MeOH 80% buffer, 14–18 min 20% MeOH 80% buffer, 18–20 min 80% buffer 20% water) with a constant flow of 1.5 mL/min, for 20 min per run. The analytes, whose retention times were determined from standards, were detected by spectrophotometry at 254.4 nm using a diode array detector (DAD).

2.12. Determination of kinetic constants

Optimal reaction parameters (pH, °T and time) were determined. Then, NAD production rate was evaluated as a function

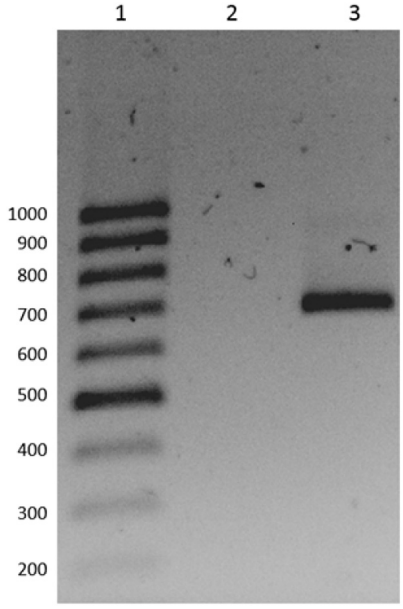

Fig. 5. **Amplification of the NMNAT coding region of *Giardia lamblia***. (1) Ladder 100 bp (fermentas). (2) Negative control (without DNA template). (3) Amplification of *glnmnat* from genomic DNA. Agarose gel in 1.5% TBE, ethidium bromide staining at 0.05%.

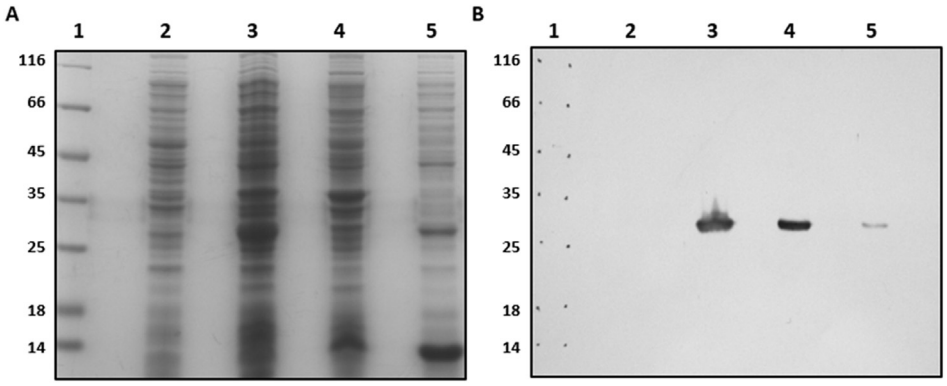

Fig. 6. **Expression of recombinant His-GlNMNAT**. (A) SDS-PAGE, Coomassie blue staining. (B) Immunoblotting on nitrocellulose membrane. (1) Molecular weight marker (MWM). (2) Uninduced BL21 cells. (3) Total cells induced. (4) Insoluble fraction. (5) Soluble fraction.

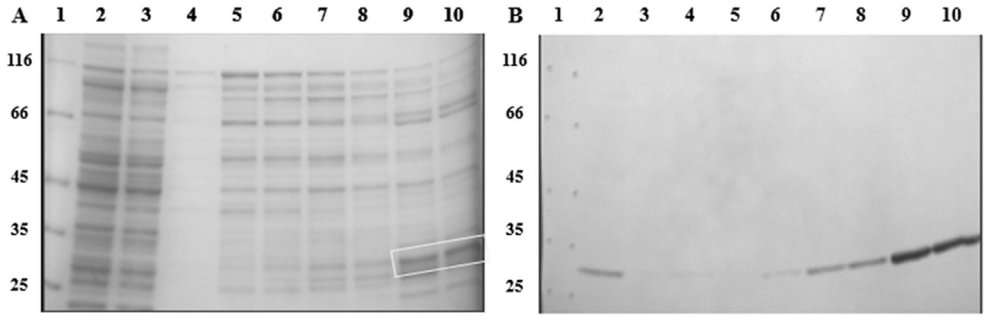

Fig. 7. **Enrichment of His-GlNMNAT recombinant protein from the soluble fraction by nickel affinity**. (A) SDS-PAGE, Coomassie blue staining. (B) Immunoblotting on nitrocellulose membrane. (1) Molecular weight marker (MWM). (2) Soluble fraction. (3) Unbound proteins. (4) Wash 15. (5,6) Eluates 50 mM Imidazole. (7,8) Eluates 80 mM Imidazole. (9,10) Eluates 250 mM Imidazole.

of substrate concentrations (ATP, NMN and NAMN). For each reaction, 1.9 μg of recombinant GlNMNAT were used. ATP concentration window: 0.2, 0.5, 0.8, 1.2, 1.5, 2, 4, 6, 8 and 10 mM, with NMN in excess (10 mM). NMN concentration window: 0.25, 0.5, 1, 2, 3, 4, 6 and 8 mM, with ATP in excess (10 mM). NAMN concentration window: 0.25, 1, 2, 3, 4, 6, 8, 10 and 12 mM, with ATP in excess (10 mM). Triplicates were done for each point in the windows. The data was processed by means of non-linear (two-parameter rectangular hyperbola) and linear regression (Hanes–Woolf). A double-reciprocal plot was made to check if the enzyme had cooperativity.

3. Results and discussion

Fig. 2 shows a multiple sequence alignment of 16 NMNATs of different organisms from which a consensus sequence of 244 aa was obtained. When searching with this sequence using BLASTP in the GiardiaDB (Giardia Assemblage A isolate WB), a sequence of 227 aa was found with a calculated size of 25.4 kDa and encoded by a coding DNA sequence (CDS) of 684 bp from chromosome 3 (Score: 75.5, E-Value: 2e-16, Gene ID: GL50803_13672/XP_001704508.1/GI:159108475, no introns, named GlNMNAT-A). Another sequence of 249 aa was identified, with a calculated size of 28.1 kDa and encoded by a CDS of 750 bp from chromosome 5 (Score: 77.4, E-value: 6e-17, Gene ID: GL50803_92618/XP_001706814.1/GI:159113174, no introns, named GlNMNAT-B). Although NMNAT identity for GlNMNAT-B has been attributed with bioinformatics tools and qualitative *in vitro* ADH-coupled enzyme tests performed by us, we have not included more information about this putative isoenzyme because it is less stable in the conditions we have tested for direct assays. For the remaining discussion, GlNMNAT-A will be considered as GlNMNAT.

Fig. 3 shows an alignment of the three human isoenzymes and the two sequences found for GlNMNAT, where the ATP motifs for recognition and binding are depicted (GxFxPx[H/T]xxH and ISSTxxR) [10]. This GlNMNAT sequences share 20–30% of identity with the human NMNATs and 28% between themselves.

The results of the CD database (conserved domains, NCBI) showed that the sequence of 227 aa has the conserved domains of nicotinamide/nicotinate mononucleotide adenylyltransferase (cd09286, E-value: 1.97e–26; cd02165, E-value: 7.03e−26). Additionally, the InterProScan 4 (EMBL-EBI) tool revealed that the protein is a possible nicotinamide mononucleotide adenylyltransferase (PTHR12039, E-value: 3.1e–124; TIGR00482, E-value: 2.7e–46). The GO (gene ontology) terms predicted were GO:0009435 (NAD biosynthetic process) and GO:0016779 (nucleotidyltransferase activity).

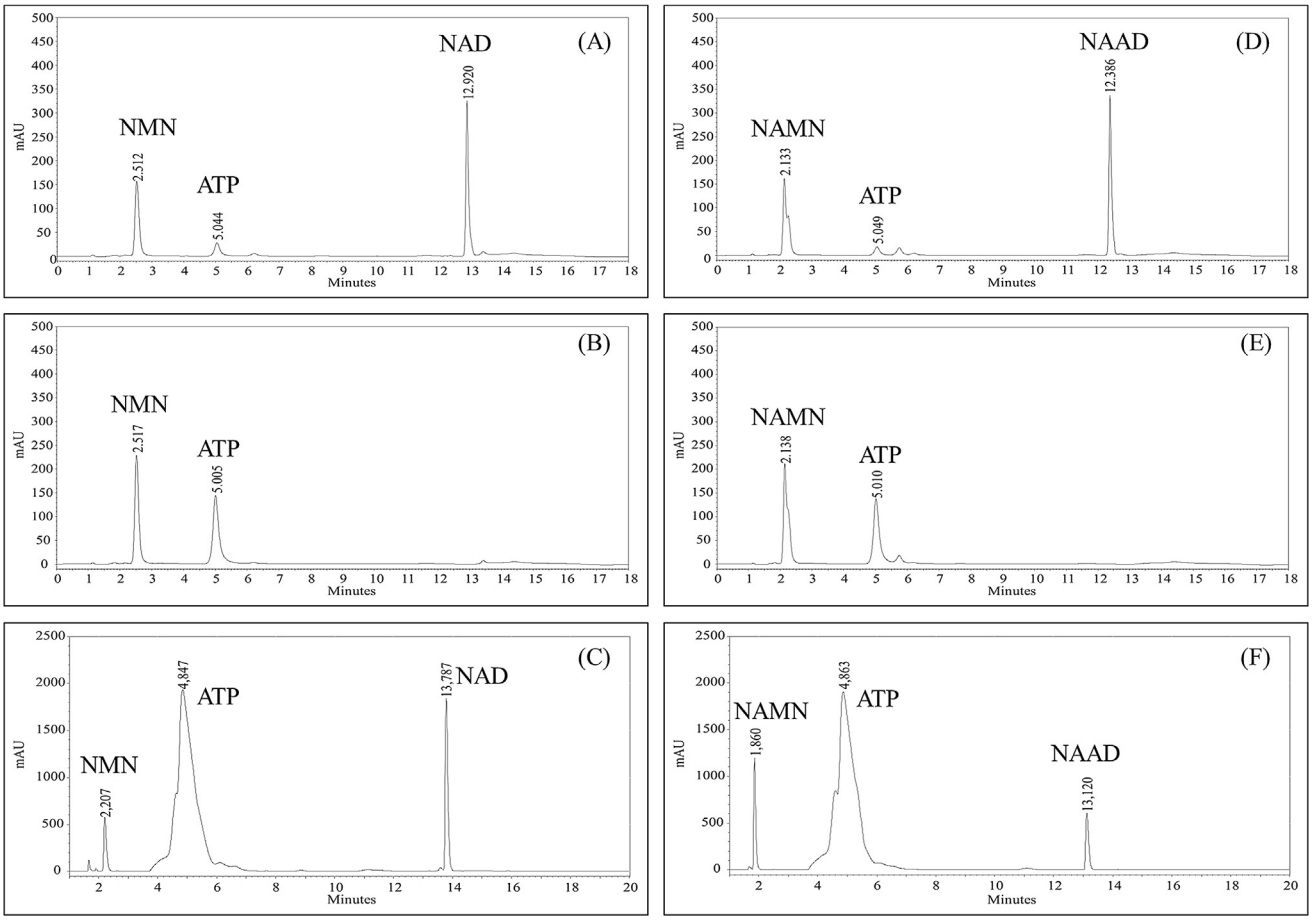

Fig. 8. **Results of a direct enzyme assay using nicotinamide mononucleotide (NMN) or nicotinic acid mononucleotide (NAMN) as a substrate. NMN: (A)** Positive control **(B)** Negative control **(C)** Reaction mixture with His-GlNMNAT. **NAMN: (D)** Positive control **(E)** Negative control **(F)** Reaction mixture with His-GlNMNAT.

Using the I-TASSER server, a tertiary structure model was built for the sequence found. Fig. 4a shows the first of the 5 models built by the server with the best quality parameters (RMSD, C-score, and TM-score). The Rossmann-type characteristic fold [22] of proteins that bind to nucleotides ($\beta\alpha\beta\alpha\beta$ motif) is observed. Fig. 4b shows a 3D alignment with the tertiary structure of HsNMNAT-3 (1nuq_A, 252 aa) generated from X-ray diffraction data (XRD) and recorded in the PDB protein structure database.

Table 2
Summary of kinetic constants for ATP and NMN.

	ATP		NMN	
	RNL	HW	RNL	HW
Km (mM)	1.48	1.54	2.53	2.72
V max (mM*min^{-1})	9.92E-02	9.82E-02	1.21E-01	1.24E-01
K cat (s^{-1})	2.44	2.41	2.97	3.04
K cat/Km (s^{-1}*mM^{-1})	1.65	1.56	1.17	1.12

NLR: non-linear regression. **HWR:** Hanes-Woolf regression. **Temperature:** 26 °C. **pH:** 7.5. **Enzyme concentration:** 6.79E-04 mM. **Enzyme activity unit:** 37.3 pkat/μg.

Several structural similarities are observed in various alpha helices and beta sheets of the overlapping proteins. Additionally, the I-TASSER server showed predictions for protein function. The EC number predicted from comparisons with proteins recorded in the databases was 2.7.7.1/18, consistent with adenylyltransferase function.

Based on the above observations, an *in vitro* characterization of the protein was performed. Fig. 5 shows the amplification of the NMNAT coding region of *Giardia lamblia* (*glnmnat*) with a size a little larger than 650 bp, which is consistent with the value of 684 bp reported in databases.

The amplified sequence was cloned into the expression vector pET100/D-TOPO, which contains the upstream sequence for the T7 promoter and is inducible with IPTG. The expressed recombinant protein is joined at its N-terminal region by a histidine tag to facilitate affinity purification and to perform immunodetection assays. Fig. 6 shows an SDS-PAGE gel and immunoblotting of the induced protein in total cell lysate and in soluble and insoluble lysate fractions produced by ultrasonic pulses. All induced fractions show a single band with a size between 25.0 and 35.0 kDa, which is consistent with the calculated size of the protein of 25.4 kDa plus 4.1 kDa from the additional 36 aa in the N-terminal region corresponding to the His-tag, the en-

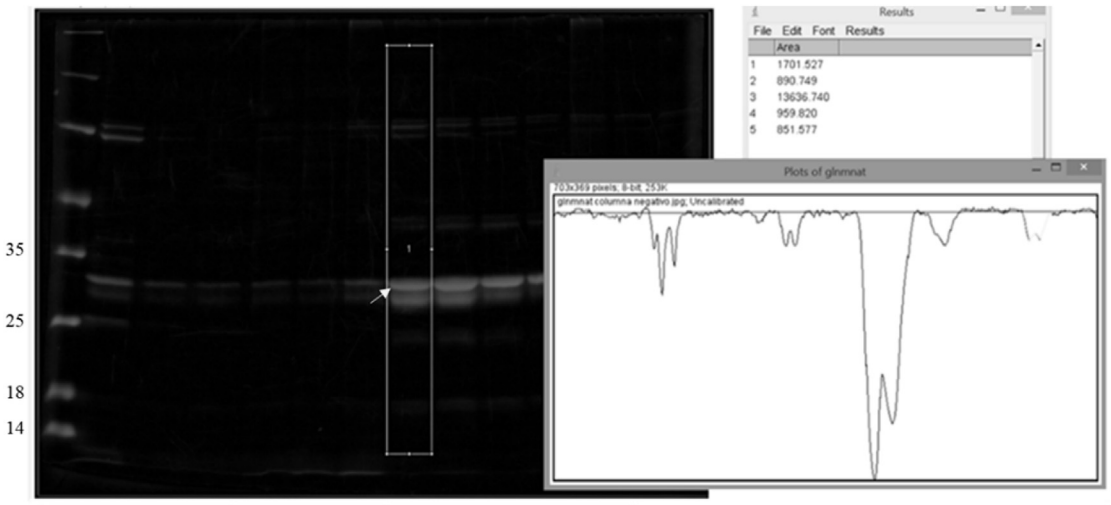

Sample	Activity pkat/ug	Enrichment (x-fold)
Soluble Fraction	0.29	--
Eluate	37.34	131

Fig. 9. **GlNMNAT enzyme preparation for kinetic experiments**. Purity estimated by means of densitometry using the Image J software. Enzyme enrichment calculated taking in account the activity of the soluble fraction and the eluate. Activity in pmol*s^{-1}*μg^{-1} or pkat*μg^{-1}.

terokinase cleavage site and the X-press epitope, for a total of 29.5 kDa. The strong band in the insoluble fraction indicates that the recombinant protein is expressed in high amounts, folding incorrectly and aggregating in great part.

Fig. 7 shows the results of the SDS-PAGE separation and the immunodetection of the recombinant protein in the different fractions obtained during partial purification from the soluble fraction. Using nickel-affinity resin, it was possible to concentrate and separate the recombinant protein from most of the other soluble proteins, with a few higher molecular weight proteins present in the eluate. The protein was specifically detected in the eluate by immunoblotting, with undetectable amounts of the protein in the washes and in unbound proteins. The eluate was used for *in vitro* activity assays to experimentally verify the adenylyltransferase function of the recombinant protein. The eluate was stored at −80 °C and supplemented with glycerol to a concentration of 20% v/v for preservation.

Fig. 8 shows the results of the direct enzyme assay using nicotinamide mononucleotide (NMN) and nicotinic acid mononucleotide (NAMN) as substrates. Adenylyltransferase activity was detected with both substrates, showing the respective production of NAD and NAAD.

Optimal pH and temperature were 7.3 and 26 °C respectively (graphs not shown). Additionally, a 30 min time was chosen for the subsequent end-point reactions (constant rate of NAD production detected between 0 and 60 min, graph not shown). For ATP and NMN, Michaelis–Menten curves were obtained, but for NAMN saturation was not observed, implying that the enzyme has low affinity yet detectable activity with this substrate *in vitro*. Double-reciprocal plots from NAD-production rates varying ATP and NMN concentrations (graphs not shown) showed no cooperativity of the enzyme. Table 2 summarizes the kinetic constants for the substrates that reached saturation. Fig. 9 shows the enzyme preparation used for the kinetic experiments, with an estimated purity of 76% based on densitometry and a 131-fold enrichment based on enzyme activity.

In comparison with the human cytosolic isoenzyme NMNAT-2, the GlNMNAT is less efficient in terms of affinity for its substrates (Km_{ATP}: 0.0889 [24], 0.107 [25], 0.204 [26]; Km_{NMN}: 0.0213 [24]) and turnover (Kcat: 8.8 [24]), hence the parasitic need of *G. lamblia* for NAD from its host despite its ability to synthesize it from NMN. Based on this, *Giardia* would use the NMN salvage pathway for NAD biosynthesis, as well as direct intake of this molecule from the host, discarding *a priori* the salvage pathway from nicotinic acid mononucleotides and the more complex kynurenine pathway for *de novo* NAAD biosynthesis which would be very demanding for such a metabolically limited organism.

4. Conclusion

From bioinformatics and experimental evidence, the identification and functional validation of nicotinamide/nicotinate mononucleotide adenylyltransferase in *Giardia lamblia* (GlNMNAT) is reported in this paper, which represents an advance in the study of the metabolism of nicotinamide and adenine dinucleotide (NAD) in *Giardia* spp.

Conflict of interest

We certify that there is no conflict of interest with any organization regarding the material discussed in the manuscript.

Acknowledgments

This work was supported by the Research Division – Bogotá. Grant number: 20429. (División de Investigación Sede Bogotá, DIB, Universidad Nacional de Colombia).

References

[1] R. Zhai, M. Rizzi, S. Garavaglia, Nicotinamide/nicotinic acid mononucleotide adenylyltransferase, new insights into an ancient enzyme, Cell. Mol. Life Sci. 66 (2009) 2805–2818.
[2] F. Berger, M.H. Ramírez-Hernández, M. Ziegler, The new life of a centenarian: signalling functions of NAD(P), Trends Biochem. Sci. 29 (2004) 111–118.
[3] B.J. North, B.L. Marshall, M.T. Borra, J.M. Denu, E. Verdin, S. Francisco, The human Sir2 ortholog, SIRT2, is an NAD(+)-dependent tubulin deacetylase, Mol. Cell. 11 (2003) 437–444 12620231.
[4] K. Ueda, ADP-Ribosylation, Ann. Rev. Biochem. 54 (1985) 73–100. http://dx.doi.org/10.1146/annurev.bi.54.070185.000445.
[5] O. Hayaishi, K. Ueda, Poly(ADP-ribose) and ADP-ribosylation of proteins, Ann. Rev. Biochem. 46 (1977) 95–116. http://dx.doi.org/10.1016/0968-0004(76)90255-3.
[6] D.L. Clapper, T.F. Walseth, P.J. Dargies, H. Cheung Lee, Pyridine nucleotide metabolites stimulate calcium release from sea urchin egg microsomes desensitized to inositol trisphosphate, J. Biol. Chem. 262 (1987) 9561–9568.
[7] F. Koch-Nolte, S. Fischer, F. Haag, M. Ziegler, Compartmentation of NAD(+)-dependent signalling, FEBS Lett. 585 (2011) 1651–1656. http://dx.doi.org/10.1016/j.febslet.2011.03.045.
[8] M. Di Stefano, L. Conforti, Diversification of NAD biological role: the importance of location, FEBS J. 280 (2013) 4711–4728. http://dx.doi.org/10.1111/febs.12433.
[9] X. Zhang, O.V. Kurnasov, S. Karthikeyan, N.V. Grishin, A.L. Osterman, H. Zhang, Structural characterization of a human cytosolic NMN/NaMN adenylyltransferase and implication in human NAD biosynthesis, J. Biol. Chem. 278 (2003) 13503–13511. http://dx.doi.org/10.1074/jbc.M300073200.
[10] F. Zhang, Q. Gu, C.J. Sih, Bioorganic chemistry of cyclic ADP-ribose (cADPR), Bioorg. Med. Chem. 7 (1999) 653–664. http://dx.doi.org/10.1016/S0968-0896(98)00256-9.
[11] C. Lau, M. Niere, M. Ziegler, The NMN/NaMN adenylyltransferase (NMNAT) protein family, Front. Biosci. 14 (2009) 410–431.
[12] R.C. Edgar, MUSCLE: multiple sequence alignment with high accuracy and high throughput, Nucleic Acids Res. 32 (2004) 1792–1797. http://dx.doi.org/10.1093/nar/gkh340.
[13] R.C. Edgar, MUSCLE: a multiple sequence alignment method with reduced time and space complexity, BMC Bioinforma. 5 (2004) 1–19. http://dx.doi.org/10.1186/1471-2105-5-113.
[14] C. Aurrecoechea, J. Brestelli, B.P. Brunk, J.M. Carlton, J. Dommer, S. Fischer, et al., GiardiaDB and TrichDB: integrated genomic resources for the eukaryotic protist pathogens Giardia lamblia and tTrichomonas vaginalis, Nucleic Acids Res. 37 (2009) D526–D530. http://dx.doi.org/10.1093/nar/gkn631.
[15] Y. Zhang, I-TASSER server for protein 3D structure prediction, BMC Bioinforma. 9 (2008) 1–8. http://dx.doi.org/10.1186/1471-2105-9-40.
[16] R. Ambrish, A. Kucukural, Y. Zhang, I-TASSER: a unified platform for automated protein structure and function prediction, Nat. Protoc. 5 (2010) 725–738. http://dx.doi.org/10.1038/nprot.2010.5.
[17] H. Lujan, Cellular biology of Giardia, Giardia a Model Org, Springer, Wien New York, 2011, pp. 141–257.
[18] J. Sambrook, D. Rusell, Molecular Cloning: a Laboratory Manual, CSHL Press, 2001.
[19] J. Walker, The Protein Protocols Handbook, second ed., Humana Press, New Jersey, USA, 2002.
[20] M. Zacharious (Ed.), Affinity Chromatography: Methods and Protocols, Humana Press, NJ, USA, 2008.
[21] E. Balducci, M. Emanuelli, N. Raffaelli, S. Ruggieri, A. Amici, G. Magni, et al., Assay methods for nicotinamide mononucleotide adenylyltransferase of wide applicability, Anal. Biochem. 228 (1995) 64–68.
[22] S. Garavaglia, I. D'Angelo, M. Emanuelli, F. Carnevali, F. Pierella, G. Magni, et al., Structure of human NMN adenylyltransferase: a key nuclear enzyme for NAD homeostasis, J. Biol. Chem. 277 (2002) 8524–8530. http://dx.doi.org/10.1074/jbc.M111589200.
[23] E.F. Pettersen, T.D. Goddard, C.C. Huang, G.S. Couch, D.M. Greenblatt, E.C. Meng, et al., UCSF chimera – a visualization system for exploratory research and analysis, J. Comput. Chem. 25 (2004) 1605–1612. http://dx.doi.org/10.1002/jcc.20084.
[24] L. Sorci, F. Cimadamore, S. Scotti, R. Petrelli, L. Cappellacci, P. Franchetti, et al., Initial-rate kinetics of human NMN-adenylyltransferases: substrate and metal ion specificity, inhibition by products and multisubstrate analogues, and isozyme contributions to NAD+ biosynthesis, Biochemistry 46 (2007) 4912–4922. http://dx.doi.org/10.1021/bi6023379.
[25] J.A. Yalowitz, S. Xiao, M.P. Biju, A.C. Antony, O.W. Cummings, M.A. Deeg, et al., Characterization of human brain nicotinamide 5′-mononucleotide adenylyltransferase-2 and expression in human pancreas, Biochem. J. 377 (2004) 317–326. http://dx.doi.org/10.1042/BJ20030518.
[26] F. Berger, C. Lau, M. Dahlmann, M. Ziegler, Subcellular compartmentation and differential catalytic properties of the three human nicotinamide mononucleotide adenylyltransferase isoforms, J. Biol. Chem. 280 (2005) 36334–36341. http://dx.doi.org/10.1074/jbc.M508660200.